Enhanced radiative transition in Si_nGe_m nanoclusters

Ming Yu,[1] C. S. Jayanthi,[1] David A. Drabold,[2] and S. Y. Wu[1]
[1]*Department of Physics, University of Louisville, Louisville, Kentucky 40292, USA*
[2]*Department of Physics and Astronomy, Condensed Matter and Surface Sciences Program, Ohio University, Athens, Ohio 45701-2979, USA*

(Received 21 January 2003; revised manuscript received 31 March 2003; published 1 July 2003)

Using an *ab initio* molecular-dynamics scheme (the "fireball" scheme), we determined the equilibrium structure of intermediate-size Si_nGe_m ($n+m=71$) nanoclusters with and without hydrogen passivation on the surface. Due to the strong surface distortion, defect states are found to permeate the energy gap of Si_nGe_m clusters. However, the defect states are removed by adding H atoms on the surface of Si_nGe_m clusters, and the gap opens up to a few eV, indicating a blueshift for photoluminescence. It is also found that the radiative transition between the highest occupied molecular orbital (HOMO) and the lowest unoccupied molecular orbital (LUMO) states is enhanced by one to two orders of magnitude for Si_nGe_m nanoclusters with respect to the corresponding pure Si clusters. This significant increase of the emission probability is attributed to the strong overlap of HOMO and LUMO wave functions centered mostly on the Ge atoms.

DOI: 10.1103/PhysRevB.68.035404 PACS number(s): 73.22.−f, 61.46.+w, 71.15.Pd, 78.67.−n

I. INTRODUCTION

The optical properties of bulk Si and Ge are rather mediocre because the light-emission in the bulk Si and Ge is a phonon-assisted indirect process. Therefore, to improve on the light-emission feature in Si-based materials is a challenge for both technological and fundamental research.

Luminescence is a result of a significant overlap in electron and hole wave functions since the strength of the luminescence (i.e., the emission rate and quantum efficiency) depends on the extent of this overlap and the transition probability. A possible means for increasing this overlap for the Si-based materials may be accomplished through, for example, alloying to change the band structure, introducing impurities to produce the intermediate state through which the electron can recombine with the hole, or zone folding to yield the desired quasidirect transition.[1] However, the most important breakthrough in this topic is the observation of visible photoluminescence (PL) from porous Si (Refs. 2–4) and Si quantum dots[5] which opens possibilities for fabricating visible light-emitting devices from Si-based materials. The structural analysis of porous Si is quite difficult. But several measurements have confirmed that the principal feature of porous Si consists of extremely fine structures which are small enough to exhibit quantum confinement effects.[2,4,5] Various theoretical works have been conducted on Si nanowires[6–10] and Si clusters.[11–15] They clarified that the quantum confinement effects give rise to a change in the electronic structure and the optical properties and they are the principle mechanism of the blueshift PL in porous Si and Si quantum dots.

Experimental reports indicated that Ge quantum dots embedded in SiO_2 glassy matrices[16] or in porous Si (Ref. 17) show a strong room-temperature luminescence. Theoretical studies on the structure and stability of Ge clusters,[18] the polarizabilities of small Ge clusters,[19] and the quantum confinement effect on excitons in Ge quantum dots[20] have also been reported. Since Ge has smaller electron and hole effective masses and a larger dielectric constant than the corresponding quantities for Si, the effective Bohr radius of the exciton in Ge is larger than that in Si, and the quantum confinement effect appears more pronounced in Ge than in Si.[16,17,20,21] These results suggest that Si_nGe_m nanoclusters could be possible candidates for components of nanoscale functional optical devices. In order to understand the physics of Si_nGe_m clusters, we performed an *ab initio* molecular-dynamics simulation for Si_nGe_m clusters of an intermediate size, and systematically studied their electronic and optical properties. There is no doubt that the mismatch effect dominating the electronic and optical properties in $Si_{1-x}Ge_x$ alloys may introduce interesting optical features in Si_nGe_m clusters. But one has to keep in mind that the surface distortion associated with stabilizing the Si_nGe_m clusters will also play an important role. Therefore the competition between the lattice mismatch and the surface distortion is the basic issue in our investigation. For this purpose, we studied Si_nGe_m clusters of an intermediate size with and without the hydrogen passivation. By comparing our results between the two sets of Si_nGe_m clusters, we found that the surface distortion plays an important role in the intermediate size of Si_nGe_m clusters but the mismatch effect dominates when Si_nGe_m clusters of the intermediate size are passivated by hydrogen atoms to eliminate the dangling bonds so as to lessen the effect of the surface distortion. We also found that the latter shows an enhancement of radiative transition and a blueshift in PL.

It should be noted that our simulations of the Si_nGe_m clusters without hydrogen passivation lead to only one of the more stable configurations among a large number of structural isomers. Hence its resulting structural and electronic properties may not exactly represent the corresponding properties of the true ground-state configuration of the Si_nGe_m clusters. However this caveat does not affect the main conclusions of our study, including the role played by the lattice

 ©2003 The American Physical Society

mismatch and the surface relaxation in Si_nGe_m clusters with and without hydrogen passivation, and the enhanced radiative transition in Si_nGe_m clusters.

II. METHOD

We considered 71-atom Si_nGe_m clusters, with m taking values 0, 18, 35, 53, and 71, respectively. The initial configurations for the five clusters were generated randomly on a regular tetrahedral network. They were then relaxed by the *ab initio* molecular- dynamics scheme developed by Sankey and co-workers (the ''fireball'' scheme).[22] This scheme is based on density-functional theory (DFT) in the local-density approximation (LDA), where a local basis set is used to construct the Kohn-Sham orbitals. The basis functions are slightly excited pseudoatomic orbitals (PAO). The Kohn-Sham orbitals are calculated self-consistently using the Hamann-Schlüter-Chiang pseudopotential[23] and the Ceperley-Alder form of the exchange-correlation potential as parametrized by Perdew and Zunger.[24] We have tested this method in the study of the strain relaxation of $Si_{1-x}Ge_x$ alloys and the results are in good agreement with the experimental observations.[25]

In our simulation, sp^3-type PAO were used with confinement radii of $5.0a_B$, $5.2a_B$, and $3.6a_B$ for Si, Ge, and H atoms, respectively. A cubic cell with a lattice constant 50 Å was chosen as the unit cell. This cell size is sufficiently large to ensure that spurious interactions between clusters will vanish. To obtain the stable configuration of a Si_nGe_m or a $Si_nGe_mH_{84}$ cluster, molecular-dynamics simulations were performed on the clusters, starting from the initial random configuration, at a temperature of 10^3 K for about 20 ps until the network was equilibrated. The network was then slowly cooled to 300 K for 5 ps, and the dynamical quenching was finally performed to fully relax the system to 0 K. Charge transfer was calculated self-consistently in the simulations, which is important in modeling clusters.

After performing the molecular-dynamical simulations, we obtained stable configurations, five each for Si_nGe_m and $Si_nGe_mH_{84}$ clusters, with the ratio $m/(n+m) = 0.0$, 0.25, 0.51, 0.75, and 1.0, respectively. As an example, Fig. 1(a) shows the stabilized configuration of the $Si_{36}Ge_{35}$ cluster. Apparently, there is strong surface distortion in this case and the stabilized structure is a compact network in a more oblate structure. This kind of structure has also been found to be more stable for the intermediate size of Si clusters from other theoretical studies.[26] It is found that the surface distortion leads to local bonding configurations with more than four bonds, in particular, in the vicinity of the surface. Further structural analysis shows that the average bond lengths of Si-Si (b_{SiSi}), Si-Ge (b_{SiGe}), and Ge-Ge (b_{GeGe}) of the Si_nGe_m clusters are expanded relative to the bulk, as shown in Fig. 2(a). But they still maintain the relationship of $b_{SiSi} < b_{SiGe} < b_{GeGe}$ and are almost independent of the ratio of $m/(n+m)$. In addition, as shown in Fig. 2(b), the average angles $\theta_{\alpha\beta\gamma}$, which show the angle between $\beta\alpha$ and $\beta\gamma$ atoms, are less than the tetrahedral angle, except for $\theta_{Si\,Si\,Si}$ in the $Si_{18}Ge_{53}$ cluster. The large fluctuation of the average angles $\theta_{\alpha\beta\gamma}$ as a function of the ratio of

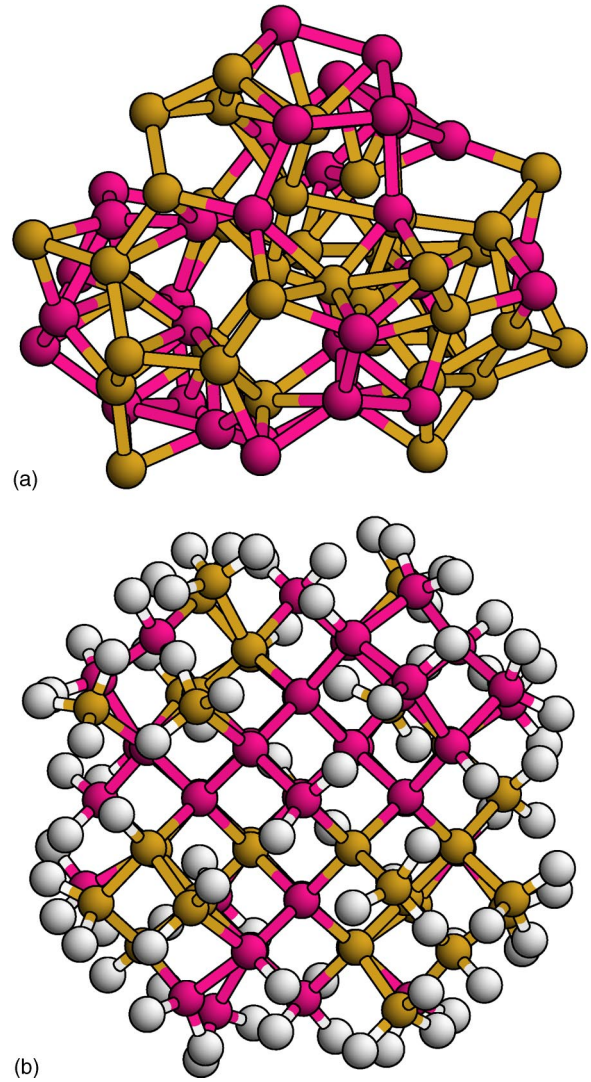

FIG. 1. The stabilized structure of the $Si_{36}Ge_{35}$ cluster shows a compact shape (a) and that of the $Si_{36}Ge_{35}H_{84}$ cluster shows a spherical-like shape with tetrahedral symmetry in the interior part (b). The Si atoms are marked by the grey color, Ge by the black, and H by the light gray.

$m/(n+m)$ indicates that the clusters have lost their initial tetrahedral symmetry. This means that the surface distortion strongly dominates in the intermediate-size Si_nGe_m clusters, whatever the ratio of Si/Ge.

When the initial configurations were passivated with 84 H atoms to terminate the dangling bonds on the surface atoms, all the relaxed $Si_nGe_mH_{84}$ clusters still maintain a tetrahedral symmetry in the interior, with only a minor distortion on the surface. Such features can be seen, for example, from the relaxed structure of $Si_{36}Ge_{35}H_{84}$ shown in Fig. 1(b). The average bond lengths b_{SiSi}, b_{SiGe}, and b_{GeGe} of the cluster [see Fig. 2(c)] and the average angles $\theta_{\alpha\beta\gamma}$ [see Fig. 2(d)] are quite close to the corresponding features in $Si_{1-x}Ge_x$ alloys [comparing Figs. 2(c) and 2(d) to Figs. 3 and 7 in Ref. 25]. This is an indication that the surface distortion in hydrogen-passivated clusters is weak even for $Si_nGe_mH_l$ clusters of an intermediate size. On the other hand, the mismatch effect

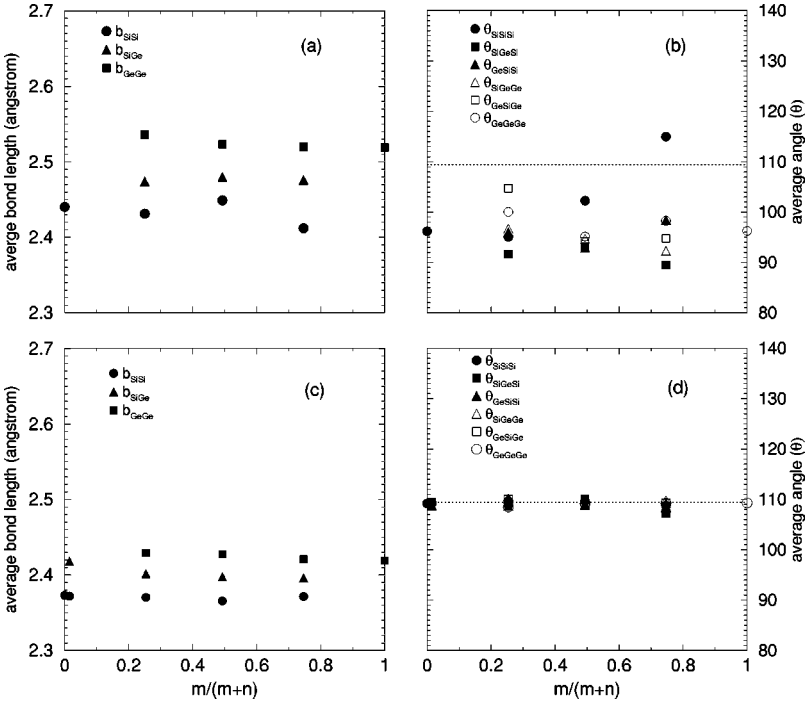

FIG. 2. The average bond lengths of b_{SiSi}, b_{SiGe}, and b_{GeGe} in Si_nGe_m clusters (a)and in $Si_nGe_mH_{84}$ clusters (c) as a function of the ratio of $m/(n+m)$. The average angles $\theta_{\alpha\beta\gamma}$ and the angle between two bonds $\beta\alpha$ and $\beta\gamma$ in Si_nGe_m clusters (b) and in $Si_nGe_mH_{84}$ clusters (d) as a function of the ratio $m/(n+m)$ are shown in the right side of the panel. The dotted lines in (b) and (d) represent the tetrahedral angle of 109.47° in bulk Si and Ge.

becomes the dominating factor in hydrogenated Si_nGe_m clusters, similar to the situation exhibited in $Si_{1-x}Ge_x$ alloys.[25]

III. ELECTRONIC STRUCTURE

The LDA calculation is known to underestimate the energy gap in the single-particle energy spectrum of semiconductor clusters. Corrections to the underestimated energy gap can be calculated using the GW approach,[14,27,28] where G refers to the Green's function and W refers to the screened interaction. However, GW calculations are expensive, even for clusters of an intermediate size considered in this work (i.e., $Si_nGe_mH_{84}$ clusters with $n+m=71$). Our main interest in this study is to provide an understanding of the trend of change in the electronic structure and optical properties of Si_nGe_m clusters of a given size as the concentration of the Ge component varies. The LDA approach is expected to be sufficiently accurate to provide a qualitative description of this trend of change. Therefore, we have calculated the electronic density of states (EDOS) of the relaxed Si_nGe_m clusters, using the same DFT/LDA scheme as that in the structural determination.

The electronic density of states of Si_nGe_m and $Si_nGe_mH_{84}$ clusters at the five ratios of $m/(n+m)$ described previously are shown in Fig. 3. From the left panel of Fig. 3, many defect states associated with the surface distortion were seen in the highest occupied molecular orbital/lowest unoccupied molecular orbital (HOMO-LUMO) energy-gap region of Si_nGe_m clusters. These defect states were cleared up when the surface was passivated by H atoms (see the right panel of Fig. 3) because H atoms terminate the dangling bonds of the surface atoms, resulting in the clusters keeping the basic tetrahedral symmetry. Even though the energy spectra of Si_nGe_m and $Si_nGe_mH_{84}$ clusters are quite different, the general feature of the energy spectrum in both cases was found to be rather insensitive to the ratio of $m/(n+m)$.

Figures 4(a) and 4(b) illustrate the HOMO-LUMO energy gap of Si_nGe_m and $Si_nGe_mH_{84}$ clusters as a function of the ratio of $m/(n+m)$, respectively. Because of the existence of the defect states in the energy-gap region, the HOMO-LUMO gap of Si_nGe_m clusters is small (only 0.4–0.5 eV) and does not show any dependence on the ratio of Si to Ge. But the HOMO-LUMO gap of the hydrogenated Si_nGe_m clusters is opened up to several eV (3.5–4.0 eV) and shows

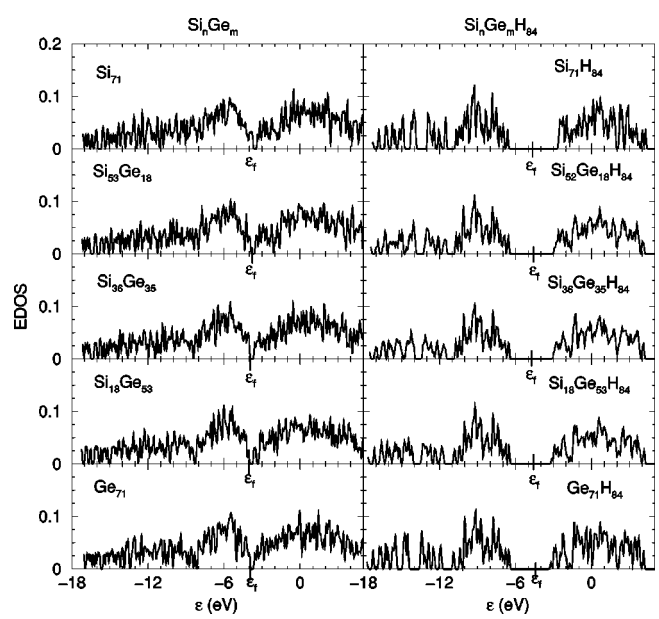

FIG. 3. The electronic densities of states of Si_nGe_m clusters (left column) and $Si_nGe_mH_{84}$ clusters (right column) at various ratios of $m/(n+m)$. The Fermi levels are denoted by the vertical bars and the broadening is 0.05 eV.

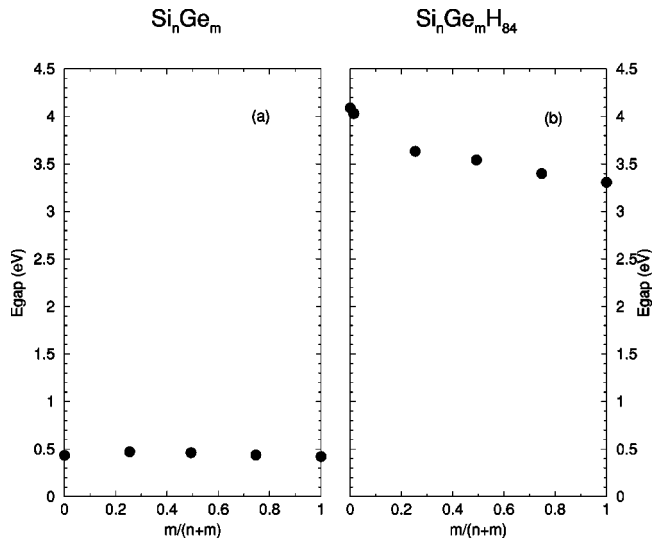

FIG. 4. The HOMO-LUMO energy gap of Si_nGe_m clusters (a) and $Si_nGe_mH_{84}$ clusters (b) as a function of the ratio of $m/(n+m)$.

a linear dependence on the ratio of Si to Ge which reflects the mismatch effect similar to that for the corresponding alloys.[25] Specifically, experimental observation[29] and theoretical calculations[30,31] indicate that the lattice mismatch associated with alloying in $Si_{1-x}Ge_x$ alloys induces a change of the conduction band, in particular, the lowest energy in the conduction band (LUMO) changes from the $\mathbf{\Delta}$ point near X point for Si-rich alloys to the L point for Ge-rich alloys,[31] leading to a nearly linear decrease of the indirect band gap. In the case of Si_nGe_m clusters passivated by hydrogen, the dominating factor is again the lattice mismatch. This similar effect is observed from the HOMO-LUMO gap as shown in Fig. 4(b). The existence of such a large energy gap for Si_nGe_m clusters of this size (with $n+m=71$) can be attributed to the effect of quantum confinement and is consistent with the scenario of a blueshift in PL.

IV. OPTICAL PROPERTIES

It is well known that an accurate calculation of the band gap is important for the determination of the optical polarizability of semiconductors and insulators. Many efforts have focused on the correction to the "too-small" band gap obtained by DFT/LDA calculations for the purpose of accurately predicting the optical response of these systems. Another key factor for determining the optical properties of these systems is a proper description of interacting electron-hole pairs (excitons). While calculations using the Green's function based on the GW approach have led to quite accurate predictions of the energy of low-lying excitations and the oscillator strength for small clusters,[32] the application of this method to clusters of intermediate sizes is still computationally too expensive. Most recently, a method based on linear-response theory within the framework of the time-dependent DFT/LDA (TDLDA) had been applied to calculate the optical spectra of clusters[13] with results in general agreement with experimental results as well as more complicated theoretical methods (e.g., the GW approach). However, at present, the application of the method is still limited to clusters of radii less than 1 nm.

The study of the dielectric function via the optical transition matrix elements allows us to obtain information directly on absorption and photoluminescence spectra. It can also allow us to obtain information indirectly on the relevant radiative PL processes. The imaginary part of the dielectric function can be calculated by[32]

$$\mathrm{Im}\epsilon(\omega)=\frac{16\pi e^2}{\omega^2}\sum_S |\hat{\mathbf{e}}\cdot\langle 0|\mathbf{v}|S\rangle|^2\delta(\omega-\Omega_S), \qquad (1)$$

where $\hat{\mathbf{e}}$ is the polarization vector of the light, $\mathbf{v}=i/\hbar[H,\mathbf{r}]$, $|0\rangle$ refers to the ground state, $|S\rangle$ the excited state, and Ω_S the excitation angular frequency. The excited state can be expanded in electron-hole pair configuration such that

$$|S\rangle=\sum_v^{\text{hole}}\sum_c^{\text{elec}} A_{vc}^S|vc\rangle. \qquad (2)$$

The coupling coefficient A_{vc}^S can be calculated within the framework of the two-particle Green's function by solving the corresponding Bethe-Salpeter equation. A reasonable approximation leads to the determination of A_{vc}^S as the positive solutions to the eigenvalue equation,[32]

$$(E_c-E_v)A_{vc}^S+\sum_{v',c'} K_{vc,v'c'}^{AA}(\Omega_S)A_{v'c'}^S=\Omega_S A_{vc}^S, \qquad (3)$$

where E_c is the single-electron energy in the conduction band, E_v the single-electron energy in the valence band, and $K_{vc,v'c'}^{AA}$ the electron-hole interaction kernel. The most computationally intensive part in the calculation is the evaluation of the electron-hole interaction kernel $K_{vc,v'c'}^{AA}$. This bottleneck is one of the main culprits that limits the application of the GW approach to only very small clusters and that of the TDLAD to clusters with radii less than 1 nm.

Using Eq. (2), the optical transition matrix elements can be written as

$$\langle 0|\mathbf{v}|S\rangle=\sum_v^{\text{hole}}\sum_c^{\text{elec}} A_{vc}^S\langle v|\mathbf{v}|c\rangle. \qquad (4)$$

The substitution of Eq. (4) into Eq. (1) shows that the imaginary part of the dielectric function depends on the transition matrix elements of electron-hole pair configuration $\langle v|\mathbf{v}|c\rangle$ as well as the coupling coefficient A_{vc}^S. For clusters Si_nGe_m of a given size ($n+m=\text{const}$), the changing composition is expected to cause more effects on the transition matrix elements $\langle v|\mathbf{v}|c\rangle$ than on the coupling coefficient A_{vc}^S because of the insensitivity of the electronic densities of state to the change in configuration [see Eq. (3) and Fig. 3]. Since the main interest of this work is to understand the effect on the optical properties of Si_nGe_m clusters of a given intermediate size ($n+m=\text{const}$) by incorporating Ge atoms into the cluster, we therefore focus our attention on the effect on $\langle v|\mathbf{v}|c\rangle$ due to the change in the composition in Si_nGe_m clusters, particularly on how the change in $\langle v|\mathbf{v}|c\rangle$ affects the radiative transition probability of the clusters as their composition varies.

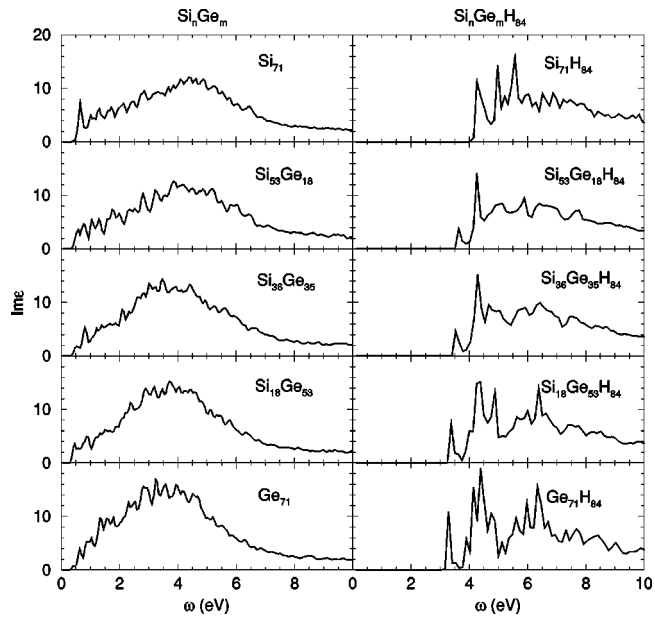

FIG. 5. The averaged imaginary part of the dielectric functions calculated from Eq. (5) of Si_nGe_m clusters (left column) and $Si_nGe_mH_{84}$ clusters (right column) at various ratio of $m/(n+m)$. The broadening is 0.05 eV.

To set up a benchmark for the analysis of the trend of the optical features of Si_nGe_m clusters of a given size but with varying compositions within the framework considered in this work, we have calculated the imaginary part of the dielectric function without the electron-hole interaction. In this situation, Eq. (1) reduces to

$$\mathrm{Im}\epsilon(\omega)=\frac{16\pi^2e^2}{V}\sum_v\sum_c|\langle v|\mathbf{r}\cdot\hat{\mathbf{e}}|c\rangle|^2\delta(E_c-E_v-\hbar\omega). \tag{5}$$

Here the sums are over all the eigenstates $|v\rangle$ and $|c\rangle$. $\mathbf{r}$ is the position operator, and V the volume of the cluster. Specifically, we calculated the average $\overline{\mathrm{Im}\epsilon(\omega)}$ $[=(16\pi^2e^2/V)\,\Sigma_v\,\Sigma_c\,\frac{1}{3}(|\langle v|x|c\rangle|^2+|\langle v|y|c\rangle|^2+|\langle v|z|c\rangle|^2)\,\delta(E_c-E_v-\hbar\omega)]$ since the shapes of the relaxed Si_nGe_m clusters are compact and suggest a more-or-less isotropic behavior.

Figure 5 presents the calculated $\overline{\mathrm{Im}\epsilon(\omega)}$ at various ratios of Si to Ge in the cases with and without H passivation. It is found that the optical gaps, defined by the onset energy of the spectral edge in Si_nGe_m clusters, are in the range 0.4–0.5 eV and are almost independent of the ratio of Si to Ge. The optical spectral peaks are smooth and broad. The spectra display low-energy transitions and show a tail near the optical edge. The tail corresponds to the defect states due to the surface distortion as shown in the EDOS of Si_nGe_m clusters (Fig. 3). Therefore, such optical properties are not suitable for application in optical devices. The optical gaps of H-terminated Si_nGe_m clusters, however, are in the range 3.3–4.1 eV and have a linear dependence on the ratio of Si to Ge. Unlike optical spectra of Si_nGe_m clusters, the spectral peaks of hydrogenated Si_nGe_m clusters are sharp with no tail at the edge of the optical spectra. Such peaks near the edge reflect the high structural symmetry (the tetrahedral symmetry in the present study) of the $Si_nGe_mH_{84}$ clusters. The large optical gaps in $Si_nGe_mH_{84}$ clusters indicate the possibility of optical applications.

TABLE I. HOMO-LUMO spontaneous emission probability W_{HL} and radiative lifetime τ_{HL} of Si_nGe_m and $Si_nGe_mH_{84}$ clusters.

System	W_{HL} (ns^{-1})	τ_{HL} (ns)
Without hydrogenation		
Si_{71}	0.164×10^{-5}	6.082×10^{5}
$Si_{53}Ge_{18}$	2.049×10^{-5}	0.488×10^{5}
$Si_{36}Ge_{35}$	1.415×10^{-5}	0.706×10^{5}
$Si_{18}Ge_{53}$	4.078×10^{-5}	0.245×10^{5}
Ge_{71}	0.824×10^{-5}	1.214×10^{5}
With hydrogenation		
$Si_{71}H_{84}$	0.0123×10^{-2}	81.362×10^{2}
$Si_{53}Ge_{18}H_{84}$	0.845×10^{-2}	1.183×10^{2}
$Si_{36}Ge_{35}H_{84}$	1.673×10^{-2}	0.598×10^{2}
$Si_{18}Ge_{53}H_{84}$	1.423×10^{-2}	0.703×10^{2}
$Ge_{71}H_{84}$	1.013×10^{-2}	0.987×10^{2}

Since the luminescence is a result of significant overlap in electron and hole wave functions, and the strength of the luminescence depends on the extent of this overlap and the transition probability, we investigated the radiative transition probabilities of Si_nGe_m and $Si_nGe_mH_{84}$ clusters. The state-to-state spontaneous transition probability (W_{ij}) (the inverse of the radiative lifetime τ_{ij}) of the first-order radiative process between states $|i\rangle$ and $|j\rangle$ is defined according to Fermi's golden rule and is given by[33]

$$W_{ij}=\frac{1}{\tau_{ij}}=\frac{4e^2\omega_{ij}^3n}{3hc^3}|\langle i|\mathbf{r}\cdot\hat{\mathbf{e}}|j\rangle|^2, \tag{6}$$

where e and m are the electron charge and mass, respectively. c is the speed of light, ω_{ij} the energy difference (divided by h) between states $|i\rangle$ and $|j\rangle$, and n the refractive index of Si_nGe_m clusters. From ellipsometry[34] and optical-absorption[3] experiments for porous Si, it seems that the refractive index decreases with increasing porosity. Since there is no measurement of the refractive index for Si_nGe_m clusters, we choose n to be 1 in the present calculation.

It is apparently from the formula of W_{ij} that the energy difference ω_{ij}^3 as well as the dipole matrix elements $\langle i|\mathbf{r}|j\rangle$ dominate the spontaneous transition probability. Table I lists the HOMO-LUMO spontaneous emission probabilities $W_{HL}[=(4e^2\omega_{HL}^3n/3hc^3)\frac{1}{3}(|\langle H|x|L\rangle|^2+|\langle H|y|L\rangle|^2+|\langle H|z|L\rangle|^2)]$ of Si_nGe_m and $Si_nGe_mH_{84}$ clusters. It can be seen that W_{HL}'s for Si_nGe_m clusters are very small ($\approx10^{-5}$ ns^{-1}). The corresponding radiative lifetimes τ_{HL} are quite large, i.e., 608 μs for Si_{71}, 49 μs for $Si_{53}Ge_{18}$, 71 μs for $Si_{36}Ge_{35}$, 25 μs for $Si_{18}Ge_{53}$, and 121 μs for Ge_{71}, respectively. But the HOMO-LUMO spontaneous transition probabilities W_{HL} of hydrogenated Si_nGe_m clusters are about two to three orders-of-magnitude larger

than the corresponding ones of Si_nGe_m clusters. Their corresponding radiative lifetimes τ_{HL} are therefore shortened by about two to three orders, i.e., 8.1 μs for $Si_{71}H_{84}$, 0.12 μs for $Si_{53}Ge_{18}H_{84}$, 0.059 μs for $Si_{36}Ge_{35}H_{84}$, 0.07 μs for $Si_{18}Ge_{53}H_{84}$, and 0.098 μs for $Ge_{71}H_{84}$, respectively. The large differences in W_{HL} and τ_{HL} between Si_nGe_m and $Si_nGe_mH_{84}$ clusters are mainly due to the energy differences of ω_{HL}^3 between HOMO-LUMO states in Si_nGe_m and $Si_nGe_mH_{84}$ clusters. As seen in Fig. 3, the HOMO-LUMO energy differences ω_{HL} of $Si_nGe_mH_{84}$ clusters are about ten times larger than those of Si_nGe_m clusters.

It is noted that the radiative lifetime τ_{HL} calculated for the $Si_{71}H_{84}$ cluster (8.1 μs) is comparable to that of the $Si_{66}H_{64}$ cluster of a similar size (6 μs) obtained by Hirao *et al.*[33] The spontaneous transition probabilities W_{HL} of the $Si_{71}H_{84}$ cluster (0.012×10^4 ms^{-1}) are also consistent with the recombination rate of an excited electron-hole pair in Si crystallites (about 10^4 ms^{-1}) for the photon energy of 4.0 eV at 5 K calculated by Delerue *et al.*[6,10] The spontaneous transition probabilities W_{HL} are found in our calculation to be higher in the pure $Ge_{71}H_{84}$ cluster (1.01×10^{-2} ns^{-1}) than in the pure $Si_{71}H_{84}$ cluster (0.012×10^{-2} ns^{-1}). This result is qualitatively consistent with the results of the radiative decay rate of excitons in Ge quantum dots (about 0.2×10^{-2} ns^{-1}) and in Si quantum dots (about 0.05×10^{-2} ns^{-1}) with the dot radius of 10 Å obtained by Takagahara and Takeda.[20]

Our analysis of the radiative transition in Si_nGe_m clusters indicates that the HOMO-LUMO spontaneous emission probability W_{HL} (radiative life-time τ_{HL}) of Si_nGe_m and $Si_nGe_mH_{84}$ clusters is very sensitive to the Ge content $[m/(n+m)]$ in the cluster. Table I shows a sudden and substantial increase in W_{HL} once Ge atoms are incorporated into the Si clusters. In particular, for hydrogen-passivated $Si_nGe_mH_{84}$ clusters, the incorporation of Ge atoms into the Si cluster can bring about a dramatic increase in W_{HL} of up to two orders of magnitude as compared to the pure hydrogen-passivated Si cluster. An increase in W_{HL} of this magnitude for $Si_nGe_mH_{84}$ with $n+m=71$ suggests that the incorporation of Ge atoms into hydrogen-passivated Si clusters may pave the way to dramatically enhance the optical properties of pure Si clusters.

To shed light on the underlying physics of this dramatic change in the HOMO-LUMO spontaneous emission probability W_{HL}, we carried out a detailed analysis of factors that might affect W_{HL}. From Eq. (6), it can be seen that W_{HL} is controlled by the interplay between the HOMO-LUMO gap ω_{HL} and the dipole matrix element $\langle H|\mathbf{r}|L\rangle$. As shown in Fig. 4, ω_{HL} for Si_nGe_m clusters of a given size does not exhibit any sensitive dependence on the Ge content. For $Si_nGe_mH_{84}$ clusters, ω_{HL} decreases with increasing Ge content $[m/(n+m)]$ and shows a linear dependence on the Ge content. However, the range of variation for ω_{HL} is only by a factor of ~1.22. On the other hand, the dependence of the dipole matrix element on $m/(n+m)$ shows a more complicated pattern (see Table II). For example, $\overline{|\langle H|\mathbf{r}|L\rangle|^2} = \frac{1}{3}(|\langle H|x|L\rangle|^2+|\langle H|y|L\rangle|^2+|\langle H|z|L\rangle|^2)$ for $Si_nGe_mH_{84}$ clusters shows a dramatic increase of two orders of magnitude once Ge atoms are incorporated into the Si cluster. It peaks at the equal composition of Si and Ge atoms, and then reduces to a smaller but equal order of magnitude for the pure Ge cluster. Since the range of variation for $\overline{|\langle H|\mathbf{r}|L\rangle|^2}$ (over two orders of magnitude) far surpasses that for ω_{HL}^3 (less than one order of magnitude), it must be the behavior of $\overline{|\langle H|\mathbf{r}|L\rangle|^2}$ that determines the pattern of behavior for W_{HL}. As shown in Table I, W_{HL} for $Si_nGe_mH_{84}$ clusters indeed exhibits a similar pattern to that of $\overline{|\langle H|\mathbf{r}|L\rangle|^2}$, namely, a drastic, almost two orders-of- magnitude, increase for a small Ge content, peaking at an equal composition of Si and Ge atoms, reducing to a somewhat smaller value for the pure hydrogen-passivated Ge cluster.

TABLE II. Dipole matrices $\overline{|\langle i|\mathbf{r}|j\rangle|^2} = \frac{1}{3}(|\langle i|x|j\rangle|^2+|\langle i|y|j\rangle|^2+|\langle i|z|j\rangle|^2)$ between HOMO-LUMO states (Å^2) of Si_nGe_m and $Si_nGe_mH_{84}$ clusters.

System	$\overline{\lvert\langle H\lvert\mathbf{r}\rvert L\rangle\rvert^2}$
Without hydrogenation	
Si_{71}	0.0329
$Si_{53}Ge_{18}$	0.322
$Si_{36}Ge_{35}$	0.238
$Si_{18}Ge_{53}$	0.791
Ge_{71}	0.181
With hydrogenation	
$Si_{71}H_{84}$	0.00294
$Si_{53}Ge_{18}H_{84}$	0.292
$Si_{36}Ge_{35}H_{84}$	0.623
$Si_{18}Ge_{53}H_{84}$	0.600
$Ge_{71}H_{84}$	0.464

To shed light on the mechanism responsible for the dramatic increase in $\overline{|\langle H|\mathbf{r}|L\rangle|^2}/W_{HL}$ once Ge atoms are incorporated into the hydrogen-passivated Si clusters, we express the dipole matrix element in terms of the pseudoatomic orbitals within the fireball scheme,[22] namely,

$$\langle H|\mathbf{r}|L\rangle = \sum_{i\alpha,j\beta} (c_{i\alpha}^H)^* c_{j\beta}^L \langle i\alpha|\mathbf{r}|j\beta\rangle, \tag{7}$$

where $c_{i\alpha}^\lambda$ denotes the coefficient of expansion of the wave function λ in the pseudoatomic orbital α at the site i. The matrix element $\langle i\alpha|\mathbf{r}|j\beta\rangle$ depends only on the structural configuration of the cluster. Specifically

$$\begin{aligned}\langle i\alpha|\mathbf{r}|j\beta\rangle &= \int \phi_\alpha^*(\mathbf{r}-\mathbf{R}_i)\mathbf{r}\phi_\beta(\mathbf{r}-\mathbf{R}_j)d\mathbf{r} \\ &= \int \phi_\alpha^*(\mathbf{r}')\mathbf{r}'\phi_\beta(\mathbf{r}'-\mathbf{R}_{ij})d\mathbf{r}' \\ &\quad +\mathbf{R}_i\int \phi_\alpha^*(\mathbf{r}')\phi_\beta(\mathbf{r}'-\mathbf{R}_{ij})d\mathbf{r}',\end{aligned} \tag{8}$$

where $\phi_\alpha(\mathbf{r}-\mathbf{R}_i)$ is the pseudoatomic orbital α centered at atomic site i, $\mathbf{R}_i$ is the position vector of atomic site i, $\mathbf{R}_{ij}=\mathbf{R}_j-\mathbf{R}_i$, and $\mathbf{r}'=\mathbf{r}-\mathbf{R}_i$, respectively.

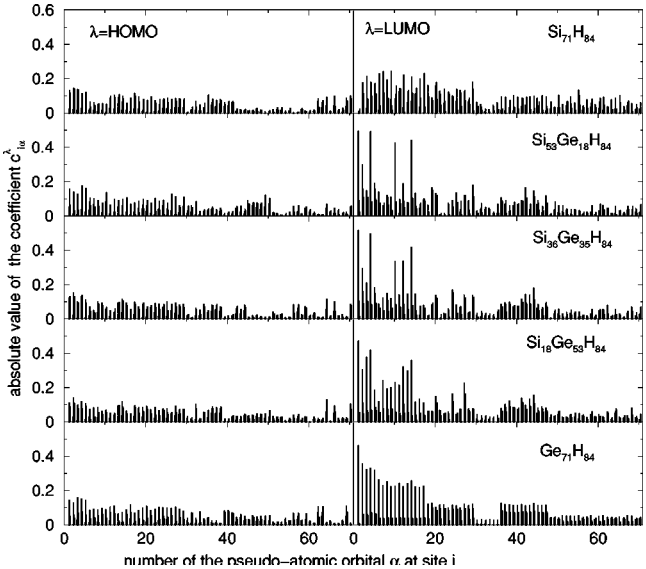

FIG. 6. The absolute value of the coefficient $c_{i\alpha}^{\lambda}$ vs the pseudo-atomic orbital α centered at atomic site i for the HOMO (left column) and LUMO states (right column) of $Si_nGe_mH_{84}$ clusters. The numbers labeled at x axis denote the number of atomic site. At each atomic site, there are four histograms corresponding to the pseudo-atomic orbital α. The order of pseudo-atomic orbital α is s, p_x, p_y, and p_z, from left to right, respectively.

Since there is no substantial structural change for hydrogen-passivated $Si_nGe_mH_l$ clusters of a given size ($n+m=\text{const}$), Eqs. (7) and (8) then indicate that the coefficients of expansion of the HOMO and LUMO states play the most significant role in determining $\langle H|\mathbf{r}|L\rangle$. In Fig. 6, we plot the absolute value of the coefficient $c_{i\alpha}^{\lambda}$ for the pseudo-atomic orbital $\phi_\alpha(\mathbf{r}-\mathbf{R}_i)$ vs atomic site i for the HOMO and LUMO states of hydrogen-passivated $Si_nGe_mH_{84}$ ($n+m=71$) clusters with various Ge contents. When the patterns of behavior for the hydrogen-passivated pure Si cluster ($Si_{71}Ge_0H_{84}$) are compared to those of the hydrogen-passivated pure Ge cluster ($Si_0Ge_{71}H_{84}$), it can be seen that the HOMO state for the two clusters shows similar distribution. However, there is a striking difference between the patterns exhibited by the LUMO states of the two clusters. In the case of the pure Si cluster, the expansion coefficients of the p_x orbital give the major contribution to the LUMO states. On the other hand, two outstanding features differentiate the pattern of the LUMO state of the pure Ge cluster from that of the pure Si cluster: (i) The expansion coefficients of the s orbital give the major contribution to the LUMO state. (ii) The magnitude of the coefficients of the s orbital is greater than that of the p_x orbital for the pure Si cluster by a factor of 2 to 3. An examination of other figures in Fig. 6 shows that the LUMO state possesses the same two features as long as the cluster has a Ge content, and these features appear mostly at the Ge sites. The overlap between an s orbital and neighboring orbitals is far less restrictive as compared to that between a p_α orbital with its neighboring orbitals. This fact, together with the more pronounced strength of the coefficients for the s orbital in the LUMO state of Ge-containing clusters, leads to a stronger overlap between the LUMO and HOMO states of Ge-containing clusters, thus explaining the correlation between the appearance of these two features and the sudden and dramatic increase in the value of $\overline{|\langle H|\mathbf{r}|L\rangle|^2}$ once Ge atoms are incorporated into the hydrogen-passivated Si clusters. This correlation also indicates that these two features are mainly responsible for the sudden and dramatic increase in W_{HL} once the hydrogen-passivated Si cluster possesses a Ge content.

Finally, it should be noted that the properties of the HOMO state are closely related to the effective mass of heavy holes while those of the LUMO state are related to the average effective mass of electrons. The mass of the heavy hole for bulk Si is reasonably close to that for bulk Ge. On the other hand, the average effective mass of electrons for bulk Ge is a factor of 2 smaller than that for bulk Si. It is therefore tempting to speculate that the behavior patterns of HOMO and LUMO states are related to the sameness of the mass of the heavy hole and the difference in the effective mass of electrons for Si and Ge, respectively. One may also reason that the fact that the effective mass of Ge is two times smaller than that of Si could be the contributing factor for the dominant contribution of the s orbital in the LUMO state for clusters with a Ge content.

V. CONCLUSION

The findings of our systematic study of the structural, electronic, and optical properties of the Si_nGe_m cluster with and without hydrogen passivation include (i) there is only a weak surface distortion in hydrogen-passivated clusters $Si_nGe_mH_l$ of intermediate sizes. The mismatch effect is then the dominating factor in determining properties of those clusters. (ii) The HOMO-LUMO gap for $Si_nGe_mH_l$ clusters of intermediate sizes opens up to several eV's, consistent with a blueshift in PL. It shows a linear dependence on the ratio $n/(n+m)$ ($n+m=\text{const}$) that is similar to the pattern exhibited by $Si_{1-x}Ge_x$ alloys.[25] (iii) The HOMO-LUMO spontaneous emission probability W_{HL} of $Si_nGe_mH_l$ clusters is very sensitive to the Ge content in the cluster. Once Ge atoms are incorporated into the cluster, this can bring about a two orders-of-magnitude increase in W_{HL}. Our analysis attributes this dramatic increase to the strong overlap between HOMO and LUMO states around Ge atoms. Our findings therefore suggest that hydrogen-passivated Si_nGe_m clusters may be viable candidates as components in optical devices.

ACKNOWLEDGMENTS

This work was supported by the NSF (Grant No. DMR-011284) and DOE (Grant No. DE-FG02-00ER4582).

[1] S. S. Lyer and Y.-H. Xie, Science **260**, 40 (1993).
[2] L. T. Canham, Appl. Phys. Lett. **57**, 1046 (1990); V. Lehman and U. Gösele, *ibid.* **58**, 56 (1991).
[3] I. Sagnes, A. Halimaoui, G. Vincent, and P. A. Badoz, Appl. Phys. Lett. **62**, 1155 (1993).
[4] P. D. Calcott, K. J. Nash, L. T. Canham, M. J. Kane, and D. Brumhead, J. Phys.: Condens. Matter **5**, L91 (1993).
[5] H. Takagi, H. Ogaea, Y. Yamazaki, A. Ishizaki, and T. Nakagiri, Appl. Phys. Lett. **56**, 2379 (1990).
[6] C. Delerue, G. Allan, and M. Lannoo, Phys. Rev. B **48**, 11 024 (1993).
[7] G. D. Sanders and Yia-Chung Chang, Phys. Rev. B **45**, 9202 (1992).
[8] F. Buda, J. Kohanoff, and M. Parrinello, Phys. Rev. Lett. **69**, 1272 (1992).
[9] Nicola A. Hill and K. Birgitta Whaley, Phys. Rev. Lett. **75**, 1130 (1995); M. Lannoo, C. Delerue, and G. Allan, *ibid.* **74**, 3415 (1995).
[10] J. P. Proot, C. Delerue, and G. Allan, Appl. Phys. Lett. **61**, 1948 (1992).
[11] B. Delley and E. F. Steigmeier, Phys. Rev. B **47**, 1397 (1993).
[12] Igor Vasiliev, Serdar Öğüt, and James R. Chelikowsky, Phys. Rev. B **65**, 115416 (2002).
[13] Igor Vasiliev, Serdar Öğüt, and James R. Chelikowsky, Phys. Rev. Lett. **86**, 1813 (2001); N. Binggeli and James R. Chelikowsky, *ibid.* **75**, 493 (1995).
[14] Serder Öğüt, James R. Chelikowsky, and Steven G. Louie, Phys. Rev. Lett. **79**, 1770 (1997).
[15] Angel Rubio, J. A. Alonso, X. Blase, L. C. Balbás, and Steven G. Louie, Phys. Rev. Lett. **77**, 247 (1996).
[16] Yoshihiko Kanemitsu, Hiroshi Uto, and Yasuki Masumoto, Appl. Phys. Lett. **61**, 2187 (1992); Yoshihito Maeda, Nobuo Tsukamoto, and Yoshiaki Yazawa, *ibid.* **59**, 3168 (1991); Yoshihito Maeda, Phys. Rev. B **51**, 1658 (1995); Masayuki Nogami and Yoshihiro Abe, Appl. Phys. Lett. **65**, 2545 (1994); Valentin Craciun and Chantal Boulmer-Leborgne, *ibid.* **69**, 1506 (1996).
[17] Feng-Qi Liu and Zhan-Guo Wang, J. Appl. Phys. **83**, 3435 (1998).
[18] Laurent Pizzagalli, Giulia Galli, John E. Klepeis, and Francois Gygi, Phys. Rev. B **63**, 165324 (2001); Serdar Öğüt and James R. Chelikowsky, *ibid.* **55**, R4914 (1997); Jijun Zhao, Jinlan Wang, and Guanghou Wang, Phys. Lett. A **275**, 281 (2000); Zhong-Yi Lu, Cai-Zhuang Wang, and Kai-Ming Ho, Phys. Rev. B **61**, 2329 (2000).
[19] Igor Vasiliev, Serdar Öğüt, and James R. Chelikowsky, Phys. Rev. Lett. **78**, 4805 (1997).
[20] Toshihide Takagahara and Kyozaburo Takeda, Phys. Rev. B **46**, 15 578 (1992).
[21] Yosuke Kayanuma, Phys. Rev. B **38**, 9797 (1988).
[22] O. F. Sankey and D. J. Niklewski, Phys. Rev. B **40**, 3979 (1989); A. A. Demkov, J. Ortega, O. F. Sankey, and M. P. Grumbach, *ibid.* **52**, 1618 (1995).
[23] D. R. Hamann, M. Schlüter, and C. Chiang, Phys. Rev. Lett. **43**, 1494 (1979).
[24] D. M. Ceperley and G. J. Alder, Phys. Rev. Lett. **45**, 566 (1980); J. Perdew and A. Zunger, Phys. Rev. B **23**, 5048 (1981).
[25] Ming Yu, C. S. Jayanthi, David A. Drabold, and S. Y. Wu, Phys. Rev. B **64**, 165205 (2001).
[26] Kai-Ming Ho, Alexander A. Shvartsburg, Bicai Pan, Zhong-Yi Lu, Cai-Zhuang Wang, Jacob G. Wacker, James L. Fye, and Martin F. Jarrold, Nature (London) **392**, 582 (1998); J. Song, Sergio E. Ulloa, and David A. Drabold, Phys. Rev. B **53**, 8042 (1996); Efthimios Kaxiras and Koblar Jackson, Phys. Rev. Lett. **71**, 727 (1993); Lubos Mitas, Jeffrey C. Grossman, Ivan Stich, and Jaroslav Tobik, *ibid.* **84**, 1479 (2000).
[27] L. Hedin, Phys. Rev. A **139**, A796 (1965); M. S. Hybertsen and S. G. Louie, Phys. Rev. B **34**, 5390 (1986); J. E. Northrup, M. S. Hybertsen, and S. G. Louie, *ibid.* **39**, 8198 (1989); R. W. Godby, M. Schlüter, and L. J. Sham, *ibid.* **37**, 10 159 (1988); M. Rohlfing, P. Krüger,and J. Pollmann, *ibid.* **48**, 17 791 (1993); *ibid.* **52**, 1905 (1995).
[28] Ming Yu, Sergio E. Ulloa, and David A. Drabold, Phys. Rev. B **61**, 2626 (2000).
[29] Rubin Braunsten, Arnold R. Moore, and Frank Herman, Phys. Rev. **109**, 695 (1958).
[30] San-Guo Shen, De-Xuan Zhang, and Xi-Oing Fan, J. Phys.: Condens. Matter **7**, 3529 (1995); Kathie E. Newman and John D. Dow, Phys. Rev. B **30**, 1929 (1984).
[31] Robert W. Jansen and Otto F. Sankey, Phys. Rev. B **36**, 6520 (1987).
[32] Michael Rohlfing and Steven G. Louie, Phys. Rev. B **62**, 4927 (2000); Phys. Rev. Lett. **80**, 3320 (1998).
[33] Masahiko Hirao, Mater. Res. Soc. Symp. Proc. **358**, 3 (1995).
[34] C. Pickering, M. I. J. Beale, D. J. Robbings, P. J. Pearson, and R. Greef, Thin Solid Films **125**, 157 (1985).